Infrared studies in free standing crystals: N_2O-doped Xe and Ar

W. G. Lawrence and V. A. Apkarian
Department of Chemistry, University of California, Irvine, California 92717

(Received March 16 1992; accepted 28 April 1992)

Infrared studies in N_2O-doped free-standing crystals of Xe and Ar are reported. N_2O isolates as monomers in Xe; however, it segregates by clustering in Ar. An anomalous temperature dependence of monomeric absorption intensities is observed in Xe, suggesting a strong guest-host electronic interaction.

I. INTRODUCTION

Rare-gas crystals grown in retractable molds, under pressure and temperature conditions that allow annealing of the solids during growth, have become known as free-standing crystals (FSC). While polycrystalline, these solids are known to have large crystal grain sizes of order 0.1 mm.[1] This property has been a main attraction for carrying out photophysical studies in doped FSC. The high optical quality and large optical pathlengths (typically 1 cm) of these solids distinguish them from matrices and make them ideally suited for such applications as solid-state laser media.[2–5] The same characteristics make FSC attractive media for spectroscopic studies of trapped species. The major disadvantage, in comparison to the well-established matrix isolation technique, is the lack of control on isolation of impurities, since the solids are grown near thermodynamic equilibrium conditions. This aspect is exemplified here by infrared studies of N_2O-doped Xe and Ar. The monomeric species is isolated in Xe but not in Ar. Nonstatistical trapping of guests is observed in a variety of systems during the course of our investigations. It is interesting to note that in some guest-host combinations, and in particular in Kr, extensive dimerization is observed without the formation of larger clusters. Cl_2-doped Kr crystals is an example which has previously been reported by us,[6] H_2S-doped Kr is another example.[7]

The main motivation behind the present studies was to use infrared absorption as a complimentary, quantitative tool to laser-induced fluorescence methods used in following the photodissociation dynamics of N_2O in crystalline Xe.[8] An anomalous behavior of absorption intensities of different vibrational modes as a function of temperature was discovered, which is reported here.

II. EXPERIMENT

The methodology used for the preparation of the free-standing crystals is similar to the one used by Rudnick *et al.*[1] Solids of approximately 1 cc volume are grown by fast deposition of a premixed gas sample onto the cold tip of a cryostat. The essential parts of the crystal growing apparatus are illustrated in Fig. 1. The crystals are grown on a copper block (OFHC) with a conical hole. The purpose of the hole is to anchor the crystal to the cold tip. A thermocouple (gold/chromel) is fed through a channel in the copper block, and centered ~ 1 mm above the tip surface into the growth zone. A Pyrex cup, 1 cm$\times$1 cm square cross section, serves as the mold for the growing crystal. The mold is fused to a $\frac{1}{4}$ in. glass tube through which the deposition gas is introduced. A double "O"-ring seal is used as the feed through for the glass tube. By sliding the tube through the "O"-ring seal, the mold is initially placed flush against the cold cryotip (~ 15 K). The gas mixture is initially introduced slowly, at a back pressure of a few Torr, until a visible seal is made between the mold and the cryotip by the frozen gas. The solid made during this period is amorphous, as judged by its snowy appearance. Once the seal is made, the back pressure is increased to 100–200 Torr, and maintained steady with a low pressure regulator. A 1 cc crystal will grow under these conditions over a period of ~ 20 min. While the cryotip temperature is maintained at ~ 15 K, as measured by a hydrogen thermometer welded to the tip, above the copper block; the growing crystal temperature is typically near 40 K (for Xe) as measured by the thermocouple embedded in the solid. After completion of growth, the gas flow is shut, and the temperature in the center of the crystal drops to 15 K. As it cools, the solid contracts, creating a gap between it and the mold surfaces. The mold is then retracted, leaving behind an optically clear, free standing crystal.

An oil diffusion pump is used to maintain vacuum in the cryostat shroud and sample manifold at high temperatures. The shroud is isolated from the pumping station once the crystal is grown, vacuum is now maintained by cryopumping alone. Samples of N_2O/Xe were prepared in a metal manifold using standard vacuum techniques. Xenon of 99.999% purity (Cryogenic Rare Gasses) and N_2O of 99.9% purity (Matheson) were used without further purification. The samples were mixed and stored in 5 l darkened glass bulbs. The large volume of the bulb prevented large changes in back pressure during crystal growth. These experiments were conducted with the head of the cryostat in the sample chamber of a Fourier transform infrared spectrometer (Nicolet 7000).

III. RESULTS

A. N_2O in xenon

Infrared spectra of N_2O-doped xenon crystals with $M/R = 10\,000$ were recorded over a range of temperatures from 16 to 45 K. The spectral resolution was usually 0.5 cm^{-1}. In some cases spectra were recorded with 0.06 cm^{-1} resolution. A representative spectrum is shown in Fig. 2. The assignment of the absorptions along with the

 0021-9606/92/162224-05$006.00

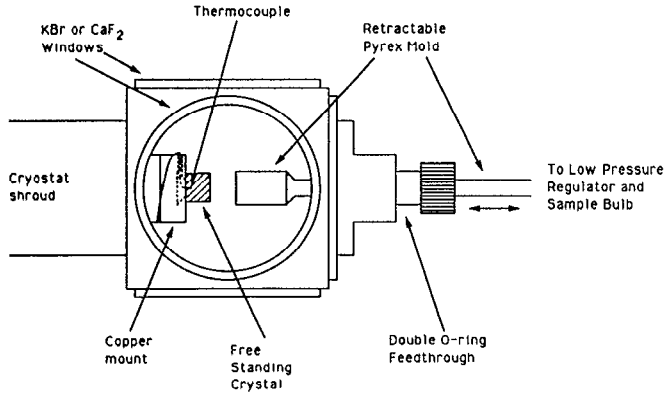

FIG. 1. Experimental arrangement used to prepare free-standing crystals (see text for details).

gas phase,[9] argon,[10,11] and nitrogen[12] matrix data, are given in Table I. The observed matrix shifts, which are also included in Table I, follow the trend in the polarizability of the host matrix. The spectra in Xe bear a striking similarity to those obtained from studies in dilute Ar matrices. In addition to monomeric features, there are absorptions to the blue of both stretches which have been previously assigned to dimers and multimers.[11] The sharp features to the red of the main bands can be assigned to ^{15}N and ^{18}O isotopes.

The absorption intensities of N_2O in xenon show an anomalous temperature dependence. The stretch fundamental absorptions become stronger as the temperature is increased from 16 to 45 K, while combination and overtone absorptions involving stretching modes show little change. In Fig. 3 the absorption profiles of the antisymmetric stretch fundamental, 001, and the first overtone of the symmetric stretch, 200, are shown at different temperatures. The area under the 001 absorption increases sixfold, while the 200 band only changes by ±20%. This temperature effect is completely reversible: upon cooling to 16 K the absorption intensities are the same as before warm up. The cluster and dimer intensities are not affected by temperature. The relative change in absorption intensities of the main bands are shown in Fig. 4(a).

The gas-phase integrated absorption intensities, S, for N_2O have been compiled by Pugh and Rao.[13] The reported numbers are for absorption at 300 K. In order to compare to the solid-state data, the gas-phase values are corrected

TABLE I. Assignments of N_2O absorptions in gas phase, matrix, and free-standing crystals of xenon.

State	Gas[a]	N_2O/Ar[b] (matrix)	N_2O/N_2[c] (matrix)	N_2O/Xe[d] (FSC)	$\Delta\nu$ (gas-Xe)
0 1 0	588.77	589.4 588.7	589.1	583.86	4.9
1 0 0	1284.9	1282.9	1291	1280.3	4.6
0 0 1	2223.76	2218.6	2235.9	2214.8	8.9
0 2 0	1168.1	1167.6	1158.2	1158.2	10.1
2 0 0	2563.3	2559.4	2567	2553	10.0
0 0 2	4417			4399.8	17.3
1 1 0	1880.3	1879.1, 1878.2	1885.9		
1 0 1	3480.8	3473.8	3499.9	3467.8	13.0
0 1 1	2798.3	2793.9, 2793.1	2809	2784.4	13.9
1 2 0	2462	2459.6	2466.9	2447.1	14.9
0 2 1	3364			3345	19.0

[a]Reference 9.
[b]Reference 11.
[c]Reference 12.
[d]Present work.

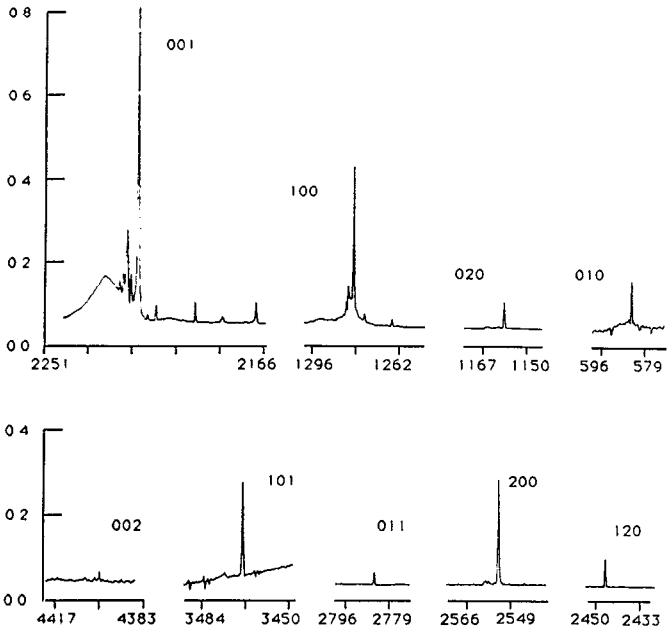

FIG. 2. Absorption spectrum of N_2O in a free standing crystal of xenon ($M/R=10\,000$; $T=15$ K). The ordinate is in absorption units. The absorption pathlength is 1 cm.

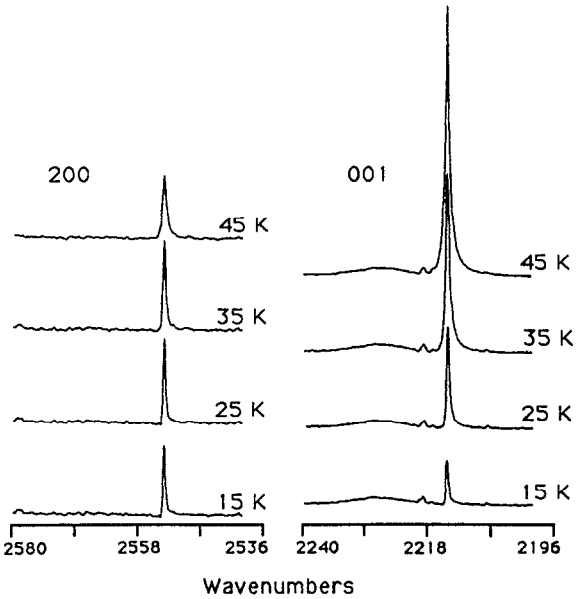

FIG. 3. Temperature dependence of the 001 and 200 modes of N_2O in a free-standing crystal of xenon ($M/R=10\,000$).

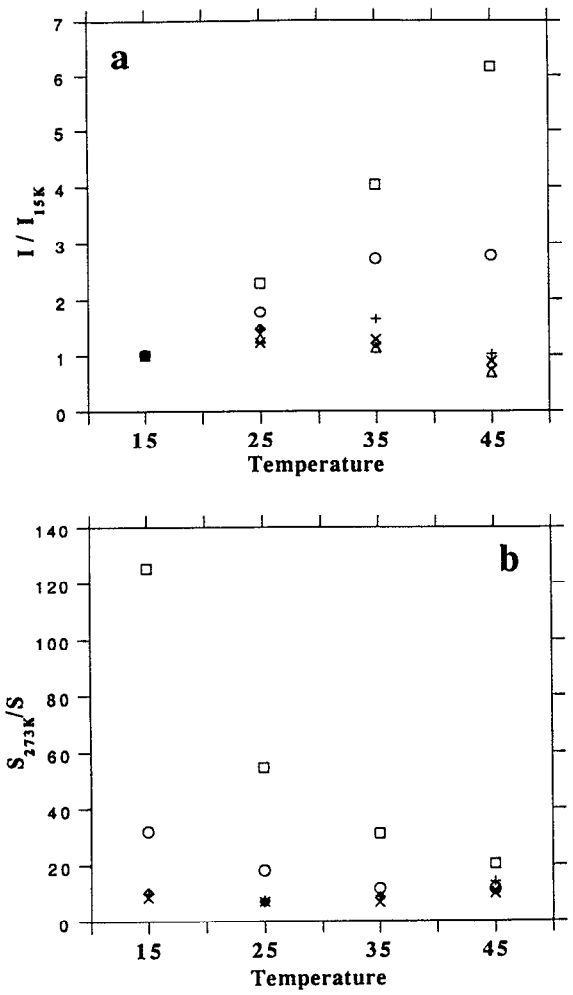

FIG. 4. (a) Temperature dependence of absorption intensities (peak heights) referenced to 15 K values for different transitions. ○=100 and 001, ◇=120, ×=200, +=101, and Δ=020) for FSC xenon. (b) Ratio of gas-phase integrated absorption intensity to the integrated absorption intensity in FSC xenon for different modes (same symbols as in a).

for the difference in temperature by taking into account the vibrational partition functions. The temperature-corrected gas-phase integrated absorption cross sections are collected in Table II. The solid-state integrated absorption cross sections are estimated as

$$S = -\Delta\nu \log(I/I_0)/2.302Nl.$$

These values are collected in Table II in units of $cm^{-2}\,atm^{-1}$. The absorption intensities in Xe are lower than those of the gas phase for all transitions. The difference is significantly larger in the case of the stretching modes, which at 15 K, are weaker than those of the gas phase by a factor of 36 and 140, respectively. At 45 K the discrepancy in these transitions become in line with all other observed absorptions, namely a factor of 10 weaker than expected. At high temperature all absorption intensities behave similarly. This is illustrated in Fig. 4(b), in which the ratio of expected and observed absorption intensities is plotted versus temperature. We emphasize that this effect is entirely reversible, as shown in Fig. 4(b). Upon cooling the 001 and 100 intensity ratios return to their respective low-temperature values.

TABLE II. Integrated absorption intensities of N_2O in gas phase and in xenon FSC (absorption intensities are given in units of $cm^{-2}\,atm^{-1}$).

State	cm^{-1}	S_g[a]	S_{Xe}[b]	S_g/S_{Xe}[c] (15 K)	S_g/S_{Xe}[c] (45 K)
0 1 0	583.86	37.3	2.12	17.6	
1 0 0	1280.3	260	7.17	36.3	13.1
0 0 1	2214.8	1977	13.97	141.6	22.9
0 2 0	1158.2	11.3	1.01	11.2	15.9
2 0 0	2553	45.2	4.66	9.7	11.0
0 0 2	4399.8	1.7	0.33	5.1	
0 1 1	2784.4	2.5	0.46	5.4	
1 0 1	3467.8	47.5	4.1	11.5	11.3
1 2 0	2447.1	11.3	0.97	11.6	14.2
0 2 1	3345				

[a]The absorption intensities from Ref. 13 with correction to 15 K.
[b]Integrated absorption intensity at 15 K.
[c]Ratio of temperature corrected gas-phase integrated absorption intensities to the integrated absorption intensities in xenon at 15 or 45 K.

B. N_2O in argon

The spectroscopy in argon was studied using the same experimental conditions and setup. Samples were prepared with M/R ratios of 9000 and 54 000. In both cases the crystals were cloudy, although less so in the more dilute sample. While the crystals were visibly scattering, no significant change was observed in the baseline level of the IR spectra. Figure 5 compares the 100 and 001 absorption bands of N_2O in xenon and argon crystals at 15 K. The bands shown are characteristic of all of the observed absorptions in that the peaks in argon crystals are much broader and are shifted to higher energies. Similarly, the bands observed in these free-standing argon crystals are also broader and blue shifted relative to those previously reported in argon matrices. The observed transitions are collected in Table III together with the Ar matrix and solid N_2O data.[14] The shifts between the present data and those of matrix Ar and solid N_2O are also included. In all cases the presently observed lines are much closer to the solid N_2O data. Note that in highly concentrated Ar matrices, $M/R = 50$, similarly shifted and broad lines have been

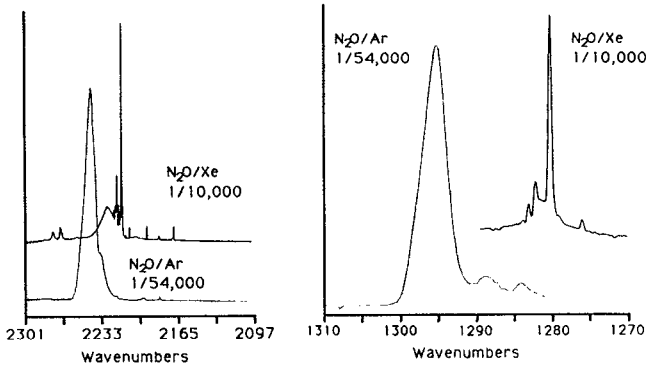

FIG. 5. Comparison of absorption profiles of the 001 and 100 modes of N_2O in FSC of argon and xenon.

TABLE III. Assignments and integrated absorption intensities of N_2O in different media.

State	Gas	N_2O/Ar^a (matrix)	N_2O/Ar (FSC)	$N_2O_{solid}{}^b$ 80K	$\Delta\nu(Ar_{FSC}-Ar_{matrix})$	$\Delta\nu(Ar_{FSC}N_2O_s)$	$S_g{}^c$	$S_{Ar}{}^d$	$S_g/S_{Ar}{}^e$
0 1 0	588.77	589.4	589.9	591	0.5	−0.1	37.3	74.4	0.50
		588.7							
1 0 0	1284.9	1282.9	1296.0	1293.4	13.1	2.6	260	357	0.72
0 0 1	2223.76	2218.6	2245.9	2238	27.3	7.9	1977	2322	0.85
0 2 0	1168.1	1167.6	1165	1165	−2.6	0	11.3	13.9	0.81
2 0 0	2563.3	2559.4	2575	2579	15.6	−4	45.2	52	0.87
0 0 2	4417		4457						
1 1 0	1880.3	1879.1							
		1878.2							
1 0 1	3480.8	3473.8	3506	3508	32.2	−2			
0 1 1	2798.3	2793.9	2813	2813	19	0			
		2793.1							
1 2 0	2462	2459.6	2470	2473	10.4	−3	11.3	8.34	1.4
0 2 1	3364		3379						

[a]Absorption wave numbers in argon matrices taken from Ref. 11.
[b]Absorption wave numbers in solid N_2O taken from Ref. 14.
[c]Temperature-corrected absorption intensities from Ref. 13.
[d]Integrated absorption intensities of N_2O in argon FSC at 15 K.
[e]Ratio of temperature-corrected gas-phase integrated absorption intensities to the integrated absorption intensities in argon FSC at 15 K.

reported. In effect, extensive aggregation of N_2O is being observed even at a dilution of $\frac{1}{54\,000}$. Although growth conditions were not systematically explored, it is possible to assert that under similar conditions, while N_2O isolates in free-standing Xe crystals, it does not in Ar.

The temperature effect observed for the monomer absorption intensities of N_2O in xenon are not observed for the N_2O aggregates in argon. Measurements were made at 15, 25, and 35 K and show identical integrated absorption intensities with the expected broadening of the peaks. The insensitivity of the absorption intensity to temperature was also observed for the small cluster peaks in xenon solids. The absolute absorption intensities of the N_2O aggregates in argon were calculated from the areas of the absorptions in $\frac{1}{54\,000}$ solids. In contrast to the absolute absorption intensities measured in xenon which, even at high temperature were a factor of 10 too small, the absorption intensities of the N_2O clusters were typically within a factor of 2 of the gas-phase values. Taking the bulk dielectric of the medium into account, the integrated absorption cross sections in solid Ar are essentially in agreement with those of the gas phase.

IV. DISCUSSION

The free-standing crystals investigated in these studies are grown subject to large thermal gradients. Although the temperature of the solid is directly measured during growth, the measurement is confined to one spot in the center of the crystal. The insulating mold makes contact with the cold tip of the cryostat, typically at 15 K; however, it also remains in contact with the vacuum shroud at room temperature. Significant mobility of species in the growth zone is therefore to be expected. As such, it is clear that isolation is only possible for commensurate guest-host pairs. The expectation that isolation probabilities will, in general, follow the trend in polarizabilities of the host Xe > Kr > Ar is obeyed with a variety of impurities in our experience. A systematic study of growth conditions has not been conducted. The case of N_2O is typical: it can be isolated in Xe while it undergoes extensive clustering and segregation in Ar.

The anomaly in absorption intensities observed in Xe and, in particular, the observed temperature-dependent intensity of certain fundamentals, to our knowledge, does not have a precedent in the matrix isolation literature. No temperature dependence of absorption intensities were observed in the most recent studies of N_2O-doped Xe matrices.[15] The prior investigations of N_2O in Ar and N_2 matrices have not commented on intensities.

The extensive overtone and combination band activity in N_2O is well known and has been treated theoretically.[16] Both mechanical and electrical anharmonicities contribute to the observed intensities of multiple quantum transitions.[17,18] A detailed force-field analysis of N_2O doped in N_2 matrices has been carried out and compared to the gas-phase parameters with the conclusion that in the solid state the main change, $\sim 1\%$, is in the harmonic force constants.[12] Anharmonicities, to cubic and quartic terms, are essentially indistinguishable between gas and N_2 matrix. We would expect that a similar picture holds in solid Xe. The gas-to-crystal Xe shifts are quite revealing in this respect. It can be seen in Table I that the shifts can be entirely ascribed to changes in the harmonic terms: Within experimental error the first overtones shift twice as much as the fundamentals and the shifts in the combinations are purely additive. Thus, based on the prior analysis in matrix N_2 and the spectral shifts in the present, and the absence of any temperature dependent spectral shifts, we conclude that the intensity anomalies cannot be ascribed to changes in anharmonicities. We therefore conclude that the inten-

sity differences are entirely due to changes in the dipole function.

The temperature dependence of the intensities seems to imply that at high temperatures, ~45 K, all intensities reach a limit yielding $S_{gas}/S_{solid} \sim 10$. This discrepancy is not understood and not likely to be due to experimental error. More interesting is the temperature dependence of intensities which is only observed for fundamentals: A threefold reduction and a tenfold reduction in intensities of 001 and 100 modes between the high-temperature limit and the 15 K values, respectively. Neither overtone nor combination bands involving the stretching modes show a significant change with temperature. This would suggest a temperature-dependent change in the first derivative of the dipole with respect to a given normal mode, $\delta\mu/\delta Q_i$. Since the fundamental intensities are related to $(\delta\mu/\delta Q_i)^2$, inferences can only be made about changes in absolute values. The signs and magnitudes of these moments, for gas phase N_2O, have been established by Brown and Person.[18] The first dipole derivatives are + and − for the 100 and 001 modes, respectively. Thus, it can be concluded that, between 45 and 15 K, $\delta\mu/\delta Q_1$ increases by a factor of ~1.7 while $\delta\mu/\delta Q_3$ decreases by a factor ~3.2. Furthermore, if we note the fact that 100 is mainly a N–O vibration while 001 is mainly an N–N vibration, then a charge redistribution in which the origin of the dipole function is shifted from N to O would be qualitatively consistent with the observation. The cavity reaction field, due to the induced dipoles on the cage atoms, is a possible source for such a shift. However, given the small dipole of N_2O ($|\mu| = 0.18$ D),[19] the magnitude of the effect is difficult to rationalize in this picture.

The model suggested earlier for the observed changes in intensities can be quantitatively tested. If we consider a Taylor expansion of μ up to second order in normal coordinates [$\mu(Q_e) = \mu_0 + \mu' Q_e + 1/2\mu'' Q_e^2$], then a shift in the origin of the dipole function, $\mu(Q_e) \rightarrow \mu(Q_e + \delta)$, would yield a change in the first moment of the function, $\delta\mu/\delta Q = \mu' + \mu''(Q_e + \delta)$, without effecting a change in the second moment. Since a complete force-field analysis of N_2O is given,[16] the expectation values of $\mu' Q_e$ and $1/2\mu'' Q_e^2$, can be directly extracted from fundamental and overtone transition intensities,[20] these are (in units of e Å) 2.8×10^{-2} and 5×10^{-2} for the 100 mode and -5.17×10^{-2} and 0.5×10^{-2} for the 001 mode of the unperturbed molecule.[20] From the observed ratios of intensities with temperature, the requisite shifts can then be calculated: $\delta/Q_e = -1.1$ and 2.5 for the 100 and 001 modes, respectively. Thus, the requisite shift in the origin of the dipole function is of the order of 1 Å and, therefore, rather difficult to rationalize by a minor perturbation.

The magnitude of the effect suggests complexation by charge transfer between N_2O and Xe (Xe···N–N–O). However, the strong temperature dependence of such an interaction seems difficult to defend. A combination of these effects, charge transfer, and reaction field of the polarized cage, associated with a tight molecule/cage alignment and arrest of librational degrees of freedom, is the most likely situation. N_2O is expected to occupy a doubly substitutional site in Xe with a rotational barrier that is insurmountable at 15 K. Reduction of its librational amplitude, concomitant with a cage compression, are the only effects expected between 45 and 15 K.

V. CONCLUSIONS

Doped free-standing crystals, while quite suitable for both photophysical and spectroscopic studies, do not yield statistical trapping of dopants. Segregation and extensive clustering are to be expected in incommensurate guest-host combinations. N_2O/Ar is an example of the latter. Due to its polarizability, Xe is a much better solvent than argon and, as such, isolation of a large selection of dopants is to be expected. N_2O isolates in Xe at M/R ratios of $\gtrsim 10\,000$.

An anomalous reduction in absorption intensities of N_2O in Xe is observed and, in particular, it is observed that the stretching fundamental intensities are temperature dependent. Possible origins of this effect are discussed; however, it has not been possible to quantify the effect with a realistic microscopic model.

ACKNOWLEDGMENTS

This research was supported by the U.S. Air Force Phillips Laboratory under Contract No. SO4611-90-K-0035, and by a grant from the National Science Foundation, ECS-8914321. A fellowship to V.A.A. by the Alfred P. Sloan Foundation is gratefully acknowledged.

[1] W. Rudnick, R. Haensel, H. Nahme, and N. Schwentner, Phys. Stat. Solidi A **87**, 319 (1985).
[2] N. Schwentner and V. A. Apkarian, Chem. Phys. Lett. **154**, 237 (1989).
[3] A. I. Katz, J. Feld, and V. A. Apkarian, Opt. Lett. **14**, 441 (1989).
[4] H. Kunttu, W. G. Lawrence, and V. A. Apkarian, J. Chem. Phys. **94**, 1692 (1991).
[5] H. Dubost, R. Charneau, M. Chergui, and N. Schwentner, J. Luminescence **48/49**, 853 (1991).
[6] G. J. Hoffman and V. A. Apkarian, J. Phys. Chem. **95**, 5372 (1991).
[7] J. Zoval, P. Ashjian, D. Imre, and V. A. Apkarian, Chem. Phys. Lett. (submitted).
[8] W. G. Lawrence and V. A. Apkarian, J. Chem. Phys. **97**, 2229 (1992).
[9] G. M. Begum and W. H. Fletcher, J. Chem. Phys. **28**, 414 (1957).
[10] L. Andrews and G. L. Johnson, J. Chem. Phys. **76**, 2875 (1982).
[11] John R. Sodeau and Robert Withnall, J. Phys. Chem. **89**, 4484 (1985).
[12] D. F. Smith, Jr., J. Overend, R. C. Spiker, and L. Andrews, Spectrochim. Acta Part A **28A**, 87 (1972).
[13] L. A. Pugh and K. N. Rao, *Intensities from Infrared Spectra* in *Molecular Spectroscopy: Modern Research Vol II*, edited by K. N. Rao (Academic, NY, 1976), pp. 165–227.
[14] David A. Dows, J. Chem. Phys. **26**, 745 (1957).
[15] H. Kreuger and E. Weitz, J. Chem. Phys. **96**, 2846 (1992).
[16] I Suzuki, J. Mol. Spectrosc. **32**, 54 (1969).
[17] R. E. Bruns and W. B. Person, J. Chem. Phys. **53**, 1413 (1970).
[18] K. G. Brown and W. B. Person, J. Chem. Phys. **xx**, 2367 (1976).
[19] S. J. Yao and J. Overend, Spectrochim. Acta A **32**, 1059 (1976).
[20] $|\langle \mu' Q_e \rangle|_s (e\,\text{Å}) = \langle 1|P_s|0\rangle = 6.5 \times 10^{-2}\{S(\text{cm}^{-2}\,\text{atm}^{-1})/\omega_s(\text{cm}^{-1})\}$; $|\langle \mu'' Q_e^2 \rangle|_s (e\,\text{Å}) = \langle 2|P_{ss}|0\rangle = 0.26\{[S(\text{cm}^{-2}\,\text{atm}^{-1})/\omega_s(\text{cm}^{-1})] - 2P_s k_{sss}/\omega_s\}$; the anharmonic force constants, k_{sss}, are taken from Ref. 15.